New imaging mapping device for the detection and location of rectal cancer

Richard Bayford[1], Andrea Bosic[2], Andrew Tizzard[1], P_Kantartzis[3], Panos Liatsis[3] and Andreas Demosthenous[4]

Middlesex University, UK[1], Dartmouth College USA[2], City University, UK[3], University College, UK[4]

r.bayford@mdx.ac.uk

Introduction

Colon and rectal cancer affects men and women equally. It is the third most common type of cancer in men, and the second most common type in women. Colon cancer usually affects people over the age of 40, with the majority of people who are diagnosed with the condition being over 60 years of age. Every year, 35 000 people are diagnosed with bowel cancer in the UK. Colorectal cancer is conventionally diagnosed by colonoscopy or barium enema examination. Colonoscopy is described as the 'gold standard' test allowing visualisation and biopsy of a potential colorectal cancer. It is, however, an invasive procedure with a degree of discomfort to the patient and has associated complication and, albeit rare, mortality rates. Double contrast barium enema x-ray has less complication risk, but has a reduced sensitivity and specificity for detecting colorectal neoplasia (benign or malignant). Double contrast enema can detect 70-80% of pre-malignant colorectal polyps that are >1 cm in diameter and a higher proportion of bowel cancers. Newer techniques such as CT colonography, whilst more acceptable to patients, has lower sensitivity and specificity compared to colonoscopy. The advent of MRI colonography has not yet been accepted into common clinical practice.

Staging of the local and distant involvement of colorectal cancer is important in planning surgical treatment and the use of adjuvant therapies prior to surgery. Whilst colon cancer and rectal cancer are similar in their aetiology and pathology, different strategies are required in staging the disease. CT scanning is now commonplace in determining distant spread of colon and rectal cancer to distant organs such as the liver and lungs. Using spiral CT, Kuszyk *et al.* achieved a sensitivity of more than 90% for detection of liver lesions larger than 1 cm in diameter and a sensitivity of 56% for detection of lesions smaller than 1 cm [1]. The accuracy of dynamic contrast-enhanced CT and of non-enhanced MR imaging in the detection of metastatic liver disease appears to be equal at 85% and the specificity of both CT (97%) and MR imaging (94%) for the detection of liver metastases also appears similar. The sensitivity of the two techniques in that study was 62% and 70%, respectively [2]. MR imaging allows detection of smaller lesions with 70% sensitivity compared to 62% for CT; however, as with CT, small lesions often lack morphologic features and cannot be definitively characterized as benign or malignant.

In rectal cancer local staging using MRI scan or endoluminal ultrasound is now common practice, rather than CT scanning, to determine the need for radiotherapy with or without chemotherapy to attempt to downstage locally-advanced rectal cancers before surgery. The accuracy of CT for local rectal cancer staging is between 65-75%, whilst lymph node disease staging is 25-73% [3], with sensitivity ranging from 22-100% and specificity from 75-100% in a number of studies. Local staging of rectal cancer with MRI has become the standard but numerous studies report disappointing figures for accuracy of the depth of mural (bowel wall) involvement between 67-86% and lymph node involvement between 57-85%. Mural staging of disease using colonoscopic EUS shows good correlation with histo-pathological stage for overall mural involvement and local lymph node stage accuracy of 92 and 65 per cent respectively [4]. In locally recurrent disease, especially rectal cancer, some patients may benefit from repeat (salvage) surgery. This is often major surgery incurring significant morbidity and mortality risk. Recently the advent of PET-CT is being used to gain more detailed knowledge of the recurrent disease locally and to determine if occult distant spread of the disease has occurred in these patients.

Colorectal/rectal cancer screening is presently being rolled-out across the UK for patients between the ages of 60 and 69 years, using faecal occult blood testing. If traces of altered blood are detected in faecal samples, patients are then offered colonoscopy. A recent campaign on the media is highlighting the important of early detection. The purpose of screening is primarily aimed at detecting pre-malignant adenomatous polyps and their subsequent removal with colonoscopy (ie: to detect and treat pre-cancerous lesions). As mentioned before, colonoscopy has a number of drawbacks as an investigative tool and more so as a screening modality. It is expensive (>=£500 per case within the NHS), uncomfortable for the patients and thus has poor compliance, as well as a real but small mortality rate.

The purpose of this paper is to report on the progress in the development of a method to locate the primary rectal tumours with bio impedance. The key aim of this project is to develop a clinically applicable device based on MfEIT imaging for diagnosis, which could map the rectal wall and hence localise the primary tumours with specificity and sensitivity that can match barium enema and colonoscopy (colonoscopy also allows tissue diagnosis by biopsy).

Method

The project consists of three parts: analysis of rectal pre-cancer cells close to the surface of the rectal wall, imaging the pre-cancer and hardware. At low frequencies, current flows only in surface mucus, and is prevented from penetrating into the tissue by the highly resistive epithelial surface. At higher frequencies, this resistance falls and current can flow freely throughout the tissue, resulting in a large reduction in transfer impedance, or 'dispersion'. The resistivity of the epithelial surface is diminished with precancerous development, and hence this dispersion becomes smaller with advancing pathology. To establish the measurement range a Tetra-polar measurement system (Zilico) was used to obtain from tissue samples obtain post surgery and measured in the pathology lab. Measurements were made at fifteen different frequencies from 76 Hz to 625 kHz. Each measurement was taken three times and averaged.

It was decided that the electrode array needed to be placed on the inside of the rectal wall and model was constructed using an FEM simulation. A simple model based on the anatomic feature of the rectum was constructed using a proprietary solid modelling package, and meshed with 38416 elements and 7652 nodes. Modelling was limited to a cylindrical region around the rectum, represented by a circular cavity axial with the mesh. A set of 8 electrodes was placed in a circular fashion around the anus.

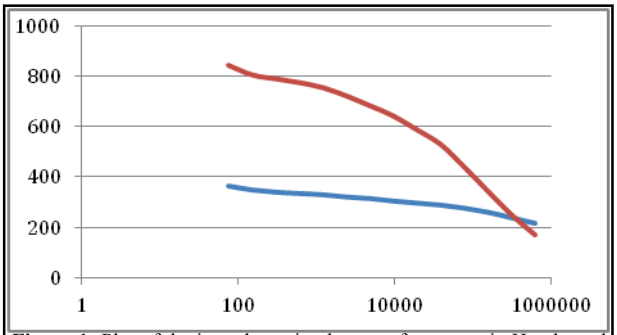

Figure 1: Plot of the impedance in ohms vs. frequency in Hz, the red line shows the tumour and the blue indicates the normal cells taken from a fresh tissue sample within one hour of the patient undergoing surgery.

Results

The plots show an example of the bio impedance measurements obtained for rectal tumour taken within the first hour of the tissue being removed from the patient. The measurements where made on normal and abnormal tissues.

Imaging

Conductivity values are reconstructed formulating the inverse problem as a non-linear least squares fitting problem with Tikhonov regularization:

$$\sigma_{rec} = \min_{\sigma} \|h(\sigma) - V\|^2 + \alpha \|L\sigma\|^2$$

where σ is the conductivity to be reconstructed $h(\sigma)$ the forward model, V, the measured voltages at the surface, resulting from current excitations, L, a regularization matrix and α the Tikhonov factor. This is a common approach in EIT reconstruction and a software package called NDRM [5] was used for solving the above inverse problem. NDRM is based on Finite Element Modeling (FEM) of the volume of interest, where a FEM mesh is used to represent the geometry of the

imaging domain, the position and extent of the electrodes, and where the same mesh is used by the software to solve for the forward fields resulting by the injection of stimulus currents. In order to model the fact that electrodes have a finite extend, resulting in a non-uniform current flow, and the presence of a contact impedance layer, NDRM implements the Complete Electrode Model [6], a set of boundary conditions that allow capturing these properties and to produce simulated measurements that can match to a high accuracy the true measured potentials at the sensing electrodes. In this application the interest is in reconstructing the conductivity distribution in circular area around the anus, and to a maximum depth of 15mm from the electrodes, as tumours typically manifest themselves in a shallow region of tissues. A sub-volume of the cylindrical mesh of a radius of 4 cm and of a thickness of 15 mm was selected as a volume where conductivity is estimated, and divided in 240 voxels, which are reconstructed as individual values of conductivity. Tetrahedra above this layer are set to a constant value of conductivity of 1 S/m, which is representative of the average conductivity value of healthy tissues. This arrangement was tested on synthetic data.

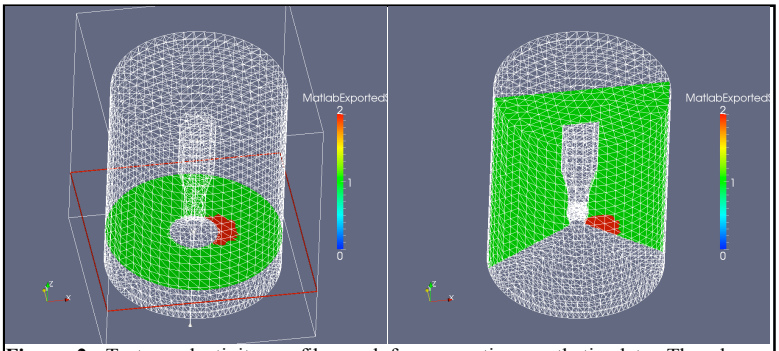

Figure 2: Test conductivity profile used for generating synthetic data. The above figures represent an axial and a sagittal cross section of the simulated conductivity distribution, where the green colour represents normal tissues (cond. 1 S/m) and the red colour abnormal tissues (cond. 2 S/m).

Fig. 2 shows a test conductivity profile which was used for generating synthetic data for image reconstruction. The axial and sagittal cross sections show background values of 1 S/m, coloured in green, and representative of normal tissues. A red inclusion, with a value of 2 S/m, representative of abnormal tissues, is generated on one side in proximity of the anus. Figure 3 shows reconstructions from synthetic data produced from the test profile of Fig. 2.

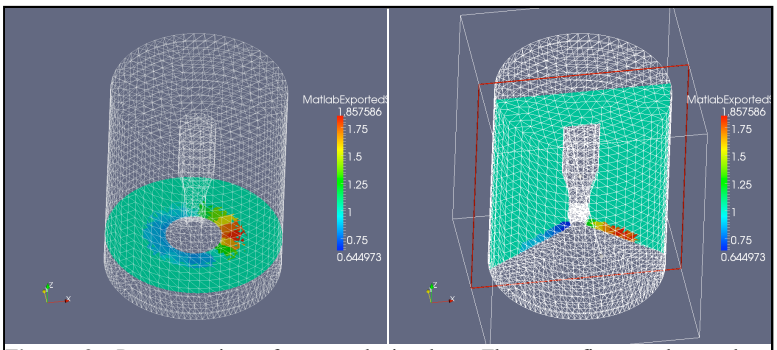

Figure 3: Reconstructions from synthetic data. The two figures above show reconstructions of the electrical resistivity distribution in a layer of 15mm of thickness from the bottom surface and of 4cm of radius. The inclusion of higher resistivity is correctly localized. The quantitative reconstructed value of 1.85 S/m for the inclusion is reasonable close to the original value of 2 S/m.

Both the axial and sagittal cross sections show that the location of the contrast is well identified, allowing in principle to detect and localized the presence of a tumour. The reconstructed conductivity value of 1.85 S/m is also quantitatively close to the original value of 2 S/m, allowing for a good ability to distinguish from healthy tissues. While these results are a positive validation of image reconstruction software and models, clinical work is currently under way to apply imaging to in-vivo experiments.

Hardware

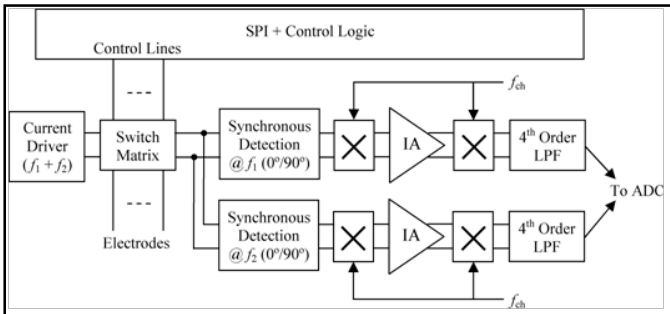

Figure 4: Basic block diagram of the integrated MfEIT system. Only two of the four analogue readout channels are shown for brevity.

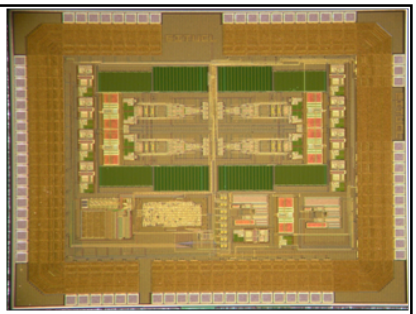

Figure 5: ASIC microphotograph.

Fig. 4 shows the simplified block diagram of the integrated MfEIT system [7]. The current driver is fully differential and exhibits large output impedance compared to the traditional Howland circuit used in EIT systems. It generates sinusoidal currents at two simultaneous frequencies, f_1 and f_2. The outputs of the current driver are used as inputs to the switch matrix, which routes the two-frequency differential current to the appropriate electrode pair. In addition, the switch matrix connects the measuring electrodes to the synchronous detection circuit. For eight electrodes, the number of measurements per frame is 40 since for each electrode pair used for current injection there are five voltage measurements to be collected. The ASIC was fabricated in 5-V, 0.6-µm CMOS technology. Figure 5 shows the chip microphotograph. The core area occupies 4.5 mm^2. The circuit operates from ±2.5 V power supplies and dissipates about 10 mW (depending on drive conditions).

In order to display the readout's capabilities both in terms of bandwidth and in terms of detecting impedance values through two frequencies applied simultaneously, a composite signal was applied at the input by summing two 20 mV p-p sinusoids at 500 kHz and at 900 kHz. Fig. 3(a) shows the input waveform and the two demodulation square waves used to lock separate channels at each frequency. In order to display the full output range for all phase values at each of the frequencies, the demodulation waveforms were applied at 500,001.5 Hz and at 900,003 Hz, respectively. In that way the phase was time varying at 1.5 Hz for the 500 kHz signal and at 3 Hz for the 900 kHz signal. The resulting outputs are cosinusoidally related to the phase and exhibit the form displayed at Fig. 6(b).

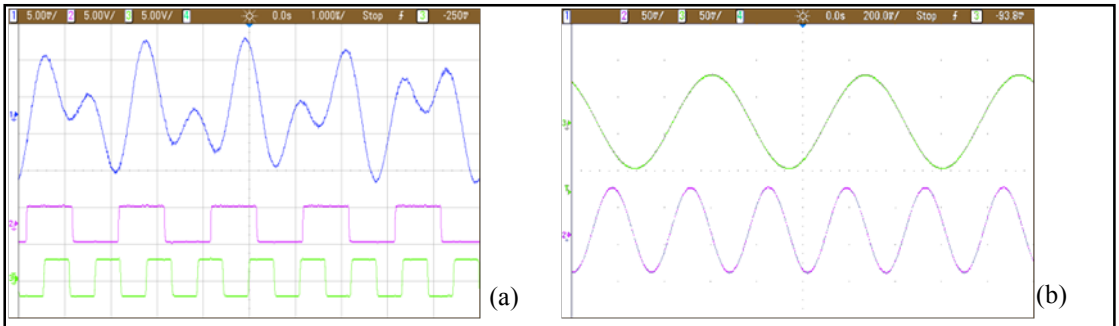
(a) (b)

Figure 6: Two frequency tests (oscillogram screen captures): (a) Input composite waveform and demodulation square waves. (b) Output variation for phase sweeping of the demodulation waveforms.

Discussion

We will present a proposed design of a new probe that could be used clinically to assess the pre-cancer site in the rectal region based on the results describe above.

References

[1] Kuszyk, B. *et al*, 1996. *Portal-phase contrast-enhanced helical CT for the detection of malignant hepatic tumors: sensitivity based on comparison with intraoperative and pathologic findings.* Am. J. Roentgenol., **166**(1) pp91-95.

[2] Horton, K.M. *et al*, 2000. *Spiral CT of Colon Cancer: Imaging Features and Role in Management.* Radiographics **20**(2) pp419-430.

[3] Mehta, S. *et al*, 1994. *Staging of colorectal cancer.* Clin.Radiol. **49**(8) pp515.

[4] Norton, S.A. & Thomas, M.G., 1999. *Staging of rectosigmoid neoplasia with colonoscopic endoluminal ultrasonography.* Br.J.Surg. **86**(7) pp942-946.

[5] Borsic, A. Hartov, A. Paulsen, K. D. Manwaring P. 2008. *3D Electric Impedance Tomography Reconstruction on Multi-Core Computing Platforms.* Proceedings IEEE EMBC'08, Vancouver.

[6] Somersalo, E. Cheney, M. Isaacson D. 1992. *Existence and uniqueness for electrode models for electric current computed tomography.* SIAM Journal on Applied Mathematics, SIAM Journal on Applied Mathematics

[7] Triantis I., Demosthenous A., Rahal M., Hong H., and Bayford R. *A multi-frequency bioimpedance measurement ASIC for electrical impedance tomography.* Proc. ESSCIRC 2011, Helsinki, Finland, Sep. 2011.

Acknowledgements: We would like to thank Zilco and Prof Brian Brown for their help with this project and the EPSRC for funding this research